

## Dimerization of endohedral fullerene in a superatomic crystal

Anastasia A. Voevodin,<sup>a</sup> Laura Abella,<sup>b</sup> Edison Castro,<sup>c</sup> Daniel W. Paley,<sup>a,d</sup> Luis M. Campos,<sup>a</sup> Antonio Rodríguez-Forteza,<sup>b</sup> Josep M. Poblet,<sup>b,\*</sup> Luis Echegoyen,<sup>c,\*</sup> and Xavier Roy<sup>a,\*</sup>

**Abstract:** We describe a solid state material created from the reaction of  $\text{Ni}_9\text{Te}_6(\text{PEt}_3)_8$  and  $\text{Lu}_3\text{N}@C_{80}$ . The resulting superatomic crystal,  $[\text{Ni}_{12}\text{Te}_{12}(\text{PEt}_3)_8]_2[(\text{Lu}_3\text{N}@C_{80})_2]$ , contains dimers of  $\text{Lu}_3\text{N}@C_{80}$  that form upon reduction of the fullerene through a single C–C bond at the triple hexagon junctions. The encapsulated  $\text{Lu}_3\text{N}$  cluster displays an unprecedented orientation that is collinear and coplanar with the inter cage carbon bond. Density functional theory calculations rationalize this unique bonding and relative orientation of the  $\text{Lu}_3\text{N}$  clusters. Our structural and theoretical results provide new insights into the effect that the  $\text{M}_3\text{N}$  cluster species has on the dimerization process of endohedral fullerenes.

The assembly of solid state materials from molecular building blocks offer significant benefits over traditional solid state reactions; the synthetic flexibility of the building blocks enables the development of functional materials with tunable properties. To this aim, fullerenes are attractive building blocks due to their exposed spherical pi-surface capable of electronic coupling in all directions. Such electronic interactions in fullerene-based materials have enabled the emergence of remarkable collective properties such as ferromagnetism and superconductivity.<sup>[1,2]</sup> Building on this foundation, our team has been developing a new class of solid state materials<sup>[3]</sup> assembled from electronically and structurally complementary molecular clusters. These materials, which we term superatomic crystals,<sup>[3-7]</sup> provide a bridge between traditional semiconductors, molecular solids, and nanocrystal arrays by combining tunability and atomic precision. Fullerenes have been particularly useful to produce collective properties in superatomic crystals, including ferromagnetic ordering,<sup>[8]</sup> coherent thermal transport<sup>[9]</sup> and semiconducting behavior.<sup>[3]</sup>

The synthetic flexibility of molecular clusters offers the possibility to create whole families of multifunctional materials by varying the constitution of the superatom building blocks. By contrast, the use of fullerenes has been, by and large, restricted to  $C_{60}$  and  $C_{70}$ . Endohedral fullerenes present the added benefit

of varying the composition of the encapsulated guest while maintaining the advantageous properties of the carbon pi-surface.<sup>[10-12]</sup> These compounds have been explored as MRI contrast reagents, electron acceptors for photovoltaic cells, and single molecule magnets.<sup>[13-15]</sup> Within the large family of endohedral fullerenes, metal nitride cluster fullerenes  $\text{M}_3\text{N}@C_{80}$  stand out due to their compositional diversity and relatively high synthetic yields.<sup>[15-17]</sup> Here we report on a new material,  $[\text{Ni}_{12}\text{Te}_{12}(\text{PEt}_3)_8]_2[(\text{Lu}_3\text{N}@C_{80})_2]$ , which we discovered during our initial exploration of the reaction involving  $\text{Ni}_9\text{Te}_6(\text{PEt}_3)_8$  and  $\text{Lu}_3\text{N}@C_{80}$ . Using single crystal x-ray diffraction (SCXRD), we find that the anionic  $\text{Lu}_3\text{N}@C_{80}$  fullerenes form dimers in this crystal. The triangular planar  $\text{Lu}_3\text{N}$  clusters inside the dimerized  $C_{80}$  cages are coplanar and collinear with the bridging C–C single bond, and point at each other. This observation contrasts with theoretical calculations<sup>[18]</sup> and a recent experimental report of  $[(\text{Sc}_3\text{N}@C_{80})_2]^{2-}$  dimers in which the clusters point away from each other.<sup>[19]</sup> To understand this unusual orientation, we complement our experimental results with density functional theory (DFT) calculations. Our results chart a clear path to assembling novel superatomic crystals from endohedral fullerenes.

When compared to  $C_{60}$  or  $C_{70}$ ,  $\text{M}_3\text{N}@C_{80}$  have lower electron affinity.<sup>[12,20,21]</sup> This presents an additional challenge for their assembly into superatomic crystals via charge transfer. To overcome this challenge, our initial plan was to react  $\text{Lu}_3\text{N}@C_{80}$  with  $\text{Ni}_9\text{Te}_6(\text{PEt}_3)_8$ , a building block with a high ionization energy.<sup>[22]</sup>

Black crystals are obtained at the interface of two solutions containing  $\text{Ni}_9\text{Te}_6(\text{PEt}_3)_8$  and  $\text{Lu}_3\text{N}@C_{80}$ , dissolved in mixtures of quinoline and toluene, and kept at  $-35^\circ\text{C}$  for seven days. SCXRD reveals that this solid is a 1:1 stoichiometric combination of a new cluster,  $\text{Ni}_{12}\text{Te}_{12}(\text{PEt}_3)_8$ , and  $\text{Lu}_3\text{N}@C_{80}$ . Refinement of the crystallographic data indicates that  $\text{Lu}_3\text{N}@C_{80}$  forms dimers and the stoichiometry of the compound is  $[\text{Ni}_{12}\text{Te}_{12}(\text{PEt}_3)_8]_2[(\text{Lu}_3\text{N}@C_{80})_2]$ . Based on previous work on superatomic crystals,<sup>[22]</sup> fullerene dimers<sup>[17,23]</sup> and endohedral fullerene dimers,<sup>[10,23]</sup> we can assign the following charges to the building blocks:  $[\text{Ni}_{12}\text{Te}_{12}(\text{PEt}_3)_8]$  and the dimer  $[(\text{Lu}_3\text{N}@C_{80})_2]$  bear 1+ and 2– charges, respectively. DFT calculations presented below agree with this assignment. Fig. 1 presents the molecular structures of  $\text{Ni}_{12}\text{Te}_{12}(\text{PEt}_3)_8$  and the dianionic  $[(\text{Lu}_3\text{N}@C_{80})_2]^{2-}$  dimer.

The cluster  $\text{Ni}_9\text{Te}_6(\text{PEt}_3)_8$  has been shown to reorganize in solution,<sup>[24]</sup> and under our reaction conditions, it produces  $\text{Ni}_{12}\text{Te}_{12}(\text{PEt}_3)_8$  (Fig. 1a). The structure of  $\text{Ni}_{12}\text{Te}_{12}(\text{PEt}_3)_8$  can be viewed as two distorted  $\text{Ni}_6$  octahedra, fused through a shared vertex. Each  $\text{Ni}_6$  octahedron contains one interstitial Ni atom. The distances separating these interstitial Ni atoms and the Ni atoms at the corner of the octahedra range from 2.40 to 2.60 Å. For comparison, the Ni–Ni distance is 2.49 Å. The other Ni–Ni

[a] A. A. Voevodin, Dr. D. W. Paley, Prof. Dr. L. Campos, Prof. Dr. X. Roy, Department of Chemistry, Columbia University, New York, New York 10027, USA, E-Mail: xr2111@columbia.edu

[b] L. Abella, Dr. A. Rodríguez-Forteza, Prof. Dr. J.M. Poblet Department de Química Física i Inorgànica, Universitat Rovira i Virgili, Marcel·lí Domingo 1, 43007-Tarragona, Spain Email: josepmaria.poblet@urv.cat

[c] E. Castro, Prof. Dr. L. Echegoyen Department of Chemistry, University of Texas at El Paso, El Paso, Texas 79968, USA. Department Email: echegoyen@utep.edu

[d] Dr. D.W. Paley Columbia Nano Initiative, Columbia University New York, NY 10027, USA.

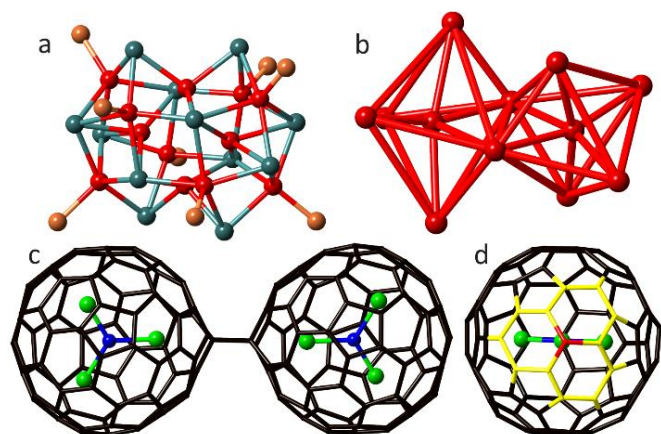


**Figure 1.** SCXRD molecular structure of (a)  $\text{Ni}_{12}\text{Te}_{12}(\text{PEt}_3)_8$ . (b) Structure of the Ni framework with distorted octahedra sharing a vertex. The Ni-Ni bonds are added to highlight the shape of the octahedra. (c)  $[\text{Lu}_3\text{N}@C_{80}]_2$  dimer, and (d)  $\text{Lu}_3\text{N}@C_{80}$  highlighting the THJ (yellow) of the inter-cage bonded carbon (red). Color code: C, black; N, blue; Lu, green; Ni, red; Te, teal and P, orange. Ethyl groups on the phosphines are removed from (a) to clarify the view.

distances are longer than 2.71 Å. The Te atoms adopt two binding modes: six Te bridge three Ni atoms and the other six Te bridge four Ni atoms. Phosphine ligands coordinate eight of the ten surface Ni atoms. The other two surface Ni atoms are bonded to four Te in a distorted tetrahedral geometry. A nickel selenide cluster with an analogous core composition,  $\text{Ni}_{12}\text{Se}_{12}(\text{PEt}_3)_6$ , was previously reported by Fenske and Ohmer<sup>[25]</sup> but the trioctahedral core of this compound is entirely different from the distorted structure of  $\text{Ni}_{12}\text{Te}_{12}(\text{PEt}_3)_8$  reported here.

The interesting result is that  $\text{Lu}_3\text{N}@C_{80}$  is dimerized in the solid state, presumably as a consequence of the electron transfer from the electron-rich superatom (Fig. 1c). Single-bonded dimers have been observed for reduced  $C_{60}$  and  $C_{70}$ , and suggested both theoretically<sup>[18]</sup> and spectroscopically<sup>[26]</sup> for endohedral fullerenes. Konarev and co-workers recently reported the first crystallographic evidence of dimerization of  $[\text{Sc}_3\text{N}@C_{80}]^-$  upon reduction with sodium fluorenone ketyl.<sup>[19]</sup> The  $\text{Sc}_3\text{N}@C_{80}$  dimer structure features significant disorder of the cages, the inter-cage C–C bond and the cluster but the orientation of the  $\text{Sc}_3\text{N}$  cluster with respect to the inter-cage C–C bond is clear and in agreement with theory: the triangular planar  $\text{Sc}_3\text{N}$  clusters are close to collinear with the bridging C–C single bond, and point away from each other.

The fully ordered structure for the  $[(\text{Lu}_3\text{N}@C_{80})_2]^{2-}$  dimer differs significantly from that of  $[(\text{Sc}_3\text{N}@C_{80})_2]^{2-}$ .<sup>[19]</sup> While the inter-cage C–C bond length (1.66(6) Å) for  $[(\text{Lu}_3\text{N}@C_{80})_2]^{2-}$  is comparable to that for  $[(\text{Sc}_3\text{N}@C_{80})_2]^{2-}$ , it selectively links the hexagon-hexagon-hexagon junctions (THJ) of neighboring  $C_{80}$  cages (Fig. 1d). This contrasts with the  $[(\text{Sc}_3\text{N}@C_{80})_2]^{2-}$  structure, in which the fullerene dimer is disordered over three positions including a mixture of THJ and PHJ dimers. More remarkably, one N–Lu bond for each  $\text{Lu}_3\text{N}$  cluster is perfectly collinear with the inter-cage C–C bond and point directly at the other  $\text{Lu}_3\text{N}$  cluster. While the  $C_{80}$  cages are fully ordered at 100 K, the  $\text{Lu}_3\text{N}$  clusters are disordered over three rotational orientations around the axis passing through the inter-cage C–C bond. The distance between the central N atom and the Lu atom closest to the inter-cage C–C

bond (2.06(2) Å) is slightly elongated, when compared to the other Lu–N bonds (2.009(19)–2.03(3) Å). The Lu–N–Lu angles are close to the ideal 120°, ranging from 117.4(9)° to 122.4(9)° and the  $\text{Lu}_3\text{N}$  cluster is almost completely flat, with the central N atom protruding from the trimetallic plane by at most 0.039(14) Å.

Fig. 2a shows the extended packing of  $[\text{Ni}_{12}\text{Te}_{12}(\text{PEt}_3)_8][\text{Lu}_3\text{N}@C_{80}]_2$ , which can be visualized as the superatomic structural analogue of the binary atomic compound rubidium peroxide,  $\text{Rb}_2\text{O}_2$ . Fig. 2b compares both structures.

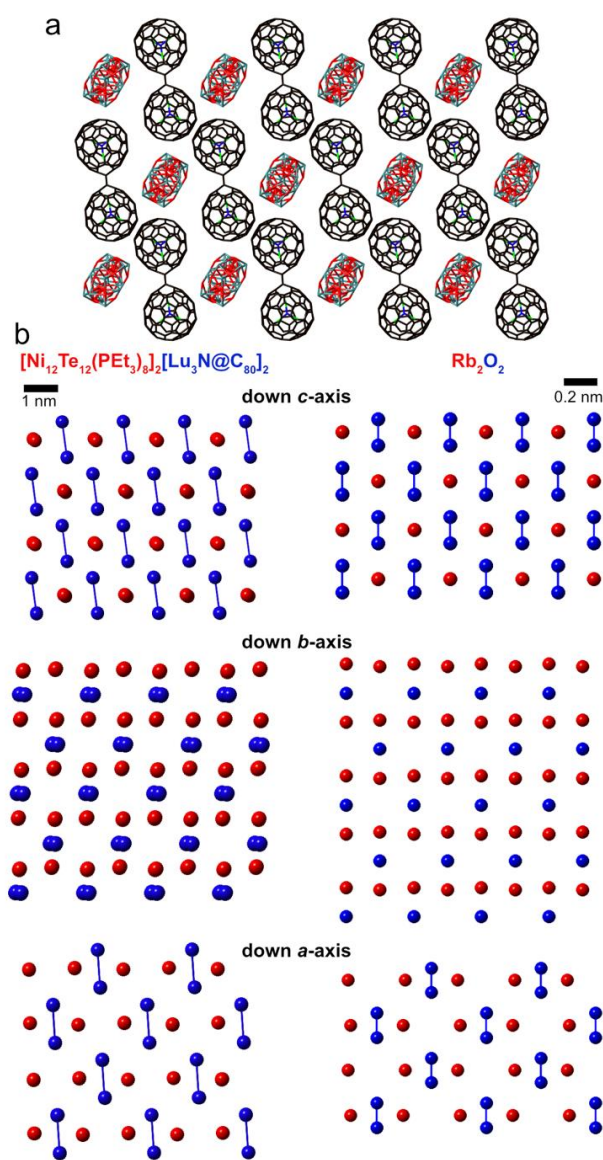


**Figure 2.** (a) Crystal packing of  $[\text{Ni}_{12}\text{Te}_{12}(\text{PEt}_3)_8][\text{Lu}_3\text{N}@C_{80}]_2$ . Color code: C, black; N, blue; Lu, green; Ni, red; and Te, teal. The phosphines on the cluster and three quinoline molecules per formula unit are removed to clarify the view. (b) Schematic views comparing the packing of  $[\text{Ni}_{12}\text{Te}_{12}(\text{PEt}_3)_8][\text{Lu}_3\text{N}@C_{80}]_2$  and  $\text{Rb}_2\text{O}_2$ .  $\text{Ni}_{12}\text{Te}_{12}(\text{PEt}_3)_8$  and  $\text{Lu}_3\text{N}@C_{80}$  are represented by blue and red dummy atoms positioned at the center of each building block, respectively. Pairs of blue atoms are linked together to denote the  $[(\text{Lu}_3\text{N}@C_{80})_2]^{2-}$  dimer and the peroxide dianion  $[\text{O}_2]^{2-}$ .

## COMMUNICATION

We present schematic views of the superstructure in which a dummy atom is positioned at the center of each building block (blue represents  $\text{Lu}_3\text{N}@C_{80}$  and red represents  $\text{Ni}_{12}\text{Te}_{12}(\text{PEt}_3)_8$ ). As with the peroxide dianion  $[\text{O}_2]^{2-}$ , pairs of blue atoms are linked together to represent the  $[(\text{Lu}_3\text{N}@C_{80})_2]^{2-}$  dimers. The packing structures of  $\text{Rb}_2\text{O}_2$  is presented looking down all three crystallographic axes, along with views showing the same orientation for the superatomic crystal. The superstructure of  $\text{Ni}_{12}\text{Te}_{12}(\text{PEt}_3)_8][(\text{Lu}_3\text{N}@C_{80})_2]$  presents a small distortion of the idealized  $\text{Rb}_2\text{O}_2$  packing resulting from a tilt of the dimer with respect to the b-axis.

The relative orientation of the  $\text{Lu}_3\text{N}$  cluster within the dimer is unexpected. In fact, the question of the relative orientation of  $\text{M}_3\text{N}$  cluster upon exohedral functionalization has received little attention in the literature. To study this question, we performed DFT calculations for a series of  $\text{M}_3\text{N}@C_{80}$  (with  $\text{M} = \text{Lu}, \text{Sc},$  and  $\text{Y}$ ) Table S3 contains the computed energy of each inter-cluster orientation upon exohedral dimerization through THJ and PHHJ junctions. Figures 3a and 3b illustrate the two possible orientations for the  $\text{M}_3\text{N}$  cluster. At the PBE/TZ2P level, the orientation in which the  $\text{Sc}_3\text{N}$  clusters are collinear, coplanar, and pointing at each other in the THJ dimer (orientation 1, Fig. 3a) is energetically disfavored by more than 10 kcal mol<sup>-1</sup> with respect to the opposite orientation in which the clusters point away from one another (orientation 2, Fig. 3b). By contrast, orientation 1 is strongly favored by 4.0 kcal mol<sup>-1</sup> in the case of the  $\text{Y}_3\text{N}$  cluster.  $\text{Lu}_3\text{N}$  is the intermediate case as Lu sits between Sc and Y in terms of size and electronegativity. DFT calculations indicate that orientation 1, which is observed experimentally, is only slightly favored by 1.3 kcal mol<sup>-1</sup> over orientation 2.

We compare the energy differences for the various types of intercage bonding (i.e. THJ-THJ, PHHJ-PHHJ and THJ-PHHJ dimers shown in Fig. 3) to understand why, unlike what has been reported for  $[(\text{Sc}_3\text{N}@C_{80})_2]^{2-}$ , the  $[(\text{Lu}_3\text{N}@C_{80})_2]^{2-}$  dimer forms exclusively through the THJ junctions.

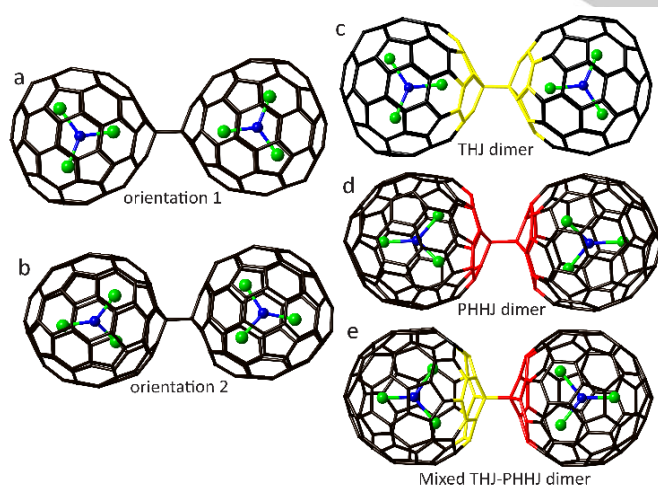


**Figure 3.** (a) and (b) Illustrations of the two possible  $\text{M}_3\text{N}$  cluster orientations in endohedral fullerene dimers, shown here linked through THJ-THJ bond. (c) THJ-THJ bonding with  $\text{Lu}_3\text{N}$  cluster in orientation 1 (d) PHHJ-PHHJ bonding with  $\text{Lu}_3\text{N}$  cluster in orientation 2, and (e) THJ-PHHJ mixed dimer with  $\text{Lu}_3\text{N}$  cluster in orientation 2.

As previously pointed out by Konarev and Popov, the energy differences between the THJ, PHHJ, and mixed THJ-PHHJ for the  $[(\text{Sc}_3\text{N}@C_{80})_2]^{2-}$  dimers computed with the PBE functional and using a continuum model solvent are small.<sup>[19]</sup> At an analogous computational level, similar results are obtained for  $[(\text{Lu}_3\text{N}@C_{80})_2]^{2-}$ : the three dimers are found within a range of only 1.1 kcal mol<sup>-1</sup>, (see Fig. 3 and Table S2). The experimentally observed THJ dimer is the lowest energy dimer for  $[(\text{Lu}_3\text{N}@C_{80})_2]^{2-}$ , with the mixed dimer almost at the same energy (0.1 kcal mol<sup>-1</sup>), followed by the symmetric PHHJ at 1.1 kcal mol<sup>-1</sup>. These very small energy differences conflict with our experimental observation that  $[\text{Ni}_{12}\text{Te}_{12}(\text{PEt}_3)_8][(\text{Lu}_3\text{N}@C_{80})_2]$  contains exclusively THJ-THJ dimers, hinting to additional contributions to the total free energy of the system such as the inclusion of the zero-point energies and/or the thermal and entropic contributions.

When these contributions are considered in the calculations, the relative free energies of THJ-PHHJ and PHHJ-PHHJ dimers increase compared to the THJ-THJ which becomes somewhat more stabilized (see Table S4). We have examined the effect of reaction temperature on each type of dimer by accounting for the zero-point energies (ZPE) and the thermal and entropic contributions in the calculations within the rigid rotor and harmonic oscillator (RRHO) approximation. The general trend is that the THJ dimer is the most abundant isomer over the whole temperature range analysed here (see Fig. S2), regardless of the density functional used.

To evaluate the relevance of the stabilizing effect of the environment around the dianion we have represented the molecular electrostatic potential (MEP) distribution of the THJ dimer with and without solvent. Notice that in a continuum solvent model, both solvent and counterion effects are included in the calculations. In both cases, the region around the inter-cage bond has the highest electron density (shown in red in Fig. S1). Fig. S1 shows that the electron density at the inter-cage junction increases significantly when the solvent environment is included in the calculation. These results suggest that the electrostatic environment surrounding the fullerenes can increase the stability of the dimer system by promoting the accumulation of electron density in the bonding hemispheres. A similar process could be at play in  $[\text{Ni}_{12}\text{Te}_{12}(\text{PEt}_3)_8][(\text{Lu}_3\text{N}@C_{80})_2]$  crystal as the cluster cations are located near the nucleophilic regions.

We computed spin density distribution for the monomeric radical anion  $[\text{Lu}_3\text{N}@C_{80}]^-$  (calculated for both THJ and PHHJ in orientation 1). In the THJ case, the C atom at the junction point holds the largest spin density while that in the PHHJ has a smaller spin density (Fig. S3) which is more distributed on the fullerene cage. In agreement with the spin density distribution, the HOMO and the LUMO of the THJ  $[\text{Lu}_3\text{N}@C_{80}]$  dimer are essentially localized on the cage, with the HOMO describing the bond formed between the two moieties (Fig. 4).

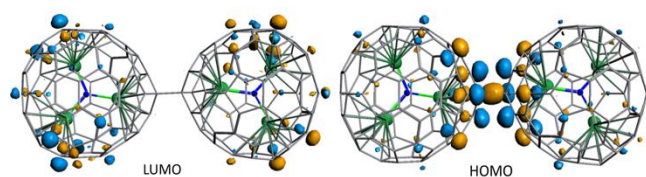


**Figure 4.** Representation of the LUMO and HOMO of the THJ  $[\text{Lu}_3\text{N}@\text{C}_{80}]_2^{2-}$  dimer with  $\text{Lu}_3\text{N}$  in orientation 1

Our results demonstrate that the nature of the encapsulated metal cluster controls the relative stability and orientation of the dimerization product. Konarev and Popov investigated the  $(\text{Sc}_3\text{N}@\text{C}_{80})_2^{2-}$  dimer through DFT calculations and found that the energy difference between the THJ and PHHJ dimers is small (less than  $2 \text{ kcal mol}^{-1}$ ), in good agreement with their experimental observation that two types of dimers are present in the crystal structure. Our calculations agree well with these results and predict that the THJ dimer becomes energetically favored for  $(\text{Lu}_3\text{N}@\text{C}_{80})_2^{2-}$  and even more so for  $(\text{Y}_3\text{N}@\text{C}_{80})_2^{2-}$ . The crystal structure of  $[\text{Ni}_{12}\text{Te}_{12}(\text{PEt}_3)_8]_2[(\text{Lu}_3\text{N}@\text{C}_{80})_2]$  reported in this communication is consistent with this first prediction.

## Acknowledgements

This work was primarily supported by the Center for Precision Assembly of Superstratic and Superatomic Solids, an NSF MRSEC (Award Number DMR-1420634). AAV thanks the NSF for GRFP (DGE-16-44869). LE and EC thank the NSF for generous support of this work under the NSF-PREM program (DMR01205302) and CHE-1408865. The Robert Welch Foundation is also gratefully acknowledged for an endowed chair to LE (grant AA-0033). We also thank the Spanish Ministry of Science and Innovation (grant CTQ2014-52774-P), the DGR of the Generalitat de Catalunya (grant 2014SGR199 and XRQTC). J.M.P. thanks the ICREA foundation for an ICREA ACADEMIA award. XR acknowledges support from the Air Force Office of Scientific Research under AFOSR Award No. FA9550-14-1-0381. Single-crystal x-ray diffraction analysis was performed at the Shared Materials Characterization Laboratory (SMCL) at Columbia University. Use of the SMCL was made possible by funding from Columbia University. We thank Prof. Craig Hawker for useful discussion.

**Keywords:** fullerenes, dimerization, cluster compounds, materials science, crystal engineering

- [1] P.-M. Allemand, K.C. Khemani, A. Koch, F. Wudl, K. Holczer, S. Donovan, *Science*, **1991**, 253, 301-302.
- [2] A. F. Hebard, M. J. Rosseinsky, R. C. Haddon, D. W. Murphy, S. H. Glarum, T. T. M. Palstra, A.P. Ramirez, A.R. Kortan, *Nature*, **1991**, 350, 600-601.
- [3] X. Roy, C. H. Lee, A. C. Crowther, C. L. Schenck, T. Besara, R. A. Lalancette, T. Siegrist, P. W. Stephens, L. E. Brus, P. Kim, M. L. Steigerwald, C. Nuckolls, *Science*, **2013**, 341, 157-160.
- [4] B. Choi, J. Yu, D. W. Paley, M. T. Trinh, M. V. Paley, J. M. Karch, A. C. Crowther, C. H. Lee, R. A. Lalancette, X. Zhu, P. Kim, M. L. Steigerwald, C. Nuckolls, X. Roy, *Nano Lett.*, **2016**, 16, 1445-1449.
- [5] A. C. R. Meichun Qian, A. Ugrinov, N. K. Chaki, S. Mandal, H. M. Saavedra, S. N. Khanna, A. Sen, P.S. Weiss, *ACS Nano*, **2010**, 4, 235-240.
- [6] S. A. Claridge, A. W. J. Castleman, S. N. Khanna, C. B. Murray, P. S. Weiss, *ACS Nano*, **2009**, 3, 244-255.
- [7] S. N. Khanna, P. Jena, *Phys. Rev. B*, **1995**, 51, 13705-13716.
- [8] C. H. Lee, L. Liu, C. Bejger, A. Turkiewicz, T. Goko, C. J. Arguello, B. A. Frandsen, S. C. Cheung, T. Medina, T. J. Munsie, R. D'Ortenzio, G. M. Luke, T. Besara, R. A. Lalancette, T. Siegrist, P. W. Stephens, A. C. Crowther, L. E. Brus, Y. Matsuo, E. Nakamura, Y. J. Uemura, P. Kim, C. Nuckolls, M. L. Steigerwald, X. Roy, *J. Am. Chem. Soc.*, **2014**, 136, 16926-16931.
- [9] W. L. Ong, E. S. O'Brien, P. S. Dougherty, D. W. Paley, C. Fred Higgs Iii, A. J. McGaughey, J. A. Malen, X. Roy, *Nat. Mater.*, **2017**, 16, 83-88.
- [10] A. A. Popov, S. Yang, L. Dunsch, *Chem. Rev.*, **2013**, 113, 5989-6113.
- [11] X. Lu, L. Feng, T. Akasaka, S. Nagase, *Chem. Soc. Rev.*, **2012**, 41, 7723-7760.
- [12] M. N. Chaur, F. Melin, A. L. Ortiz, L. Echegoyen, *Angew. Chem. Int. Ed.*, **2009**, 48, 7514-7538.
- [13] B. Náfrádi, Á. Antal, Á. Pásztor, L. Forró, L. F. Kiss, T. Fehér, É. Kováts, S. Pekker, A. Jánossy, *J. Phys. Chem. Lett.*, **2012**, 3, 3291-3296.
- [14] S. Sato, S. Seki, G. Luo, M. Suzuki, J. Lu, S. Nagase, T. Akasaka, *J. Am. Chem. Soc.*, **2012**, 134, 11681-11686.
- [15] F. F. Li, A. Rodriguez-Forteza, J. M. Poblet, L. Echegoyen, *J. Am. Chem. Soc.*, **2011**, 133, 2760-2765.
- [16] C.M. Cardona, L. Echegoyen, *J. Am. Chem. Soc.*, **2005**, 127, 10448-10453.
- [17] L. Echegoyen, L.E. Echegoyen, *Acc. Chem. Res.*, **1998**, 31, 593-601.
- [18] A. A. Popov, S. M. Avdoshenko, G. Cuniberti, L. Dunsch, *J. Phys. Chem. Lett.*, **2011**, 2, 1592-1600.
- [19] D. V. Konarev, L. V. Zorina, S. S. Khasanov, A. A. Popov, A. Otsuka, H. Yamochi, G. Saito and R. N. Lyubovskaya, *Chem. Commun.*, **2016**, 52, 10763-10766.
- [20] H. Ueno, S. Aoyagi, Y. Yamazaki, K. Ohkubo, N. Ikuma, H. Okada, T. Kato, Y. Matsuo, S. Fukuzumi, K. Kokubo, *Chem. Sci.*, **2016**, 7, 5770-5774.
- [21] A. A. Popov, L. Dunsch, *J. Phys. Chem. Lett.*, **2011**, 2, 786-794.
- [22] V. Chauhan, S. Sahoo, and S. N. Khanna, *J. Am. Chem. Soc.*, **2016**, 138, 1916-1921.
- [23] J.L. Segura, and N. Martin, *Chem. Soc. Rev.*, **2000**, 29, 13-25.
- [24] J.G. Brennan, T. Siegrist, S.M. Stuczynski, and M.L. Steigerwald, *J. Am. Chem. Soc.*, **1989**, 111, 9240-9241.
- [25] D. Fenske and J. Ohmer, *Angew. Chem. Int. Ed.*, **1987**, 26, 148-151.
- [26] T. Huang, J. Zhao, M. Feng, H. Petek, S. Yang, L. Dunsch, *Phys. Rev. B*, **2010**, 81, 085434.

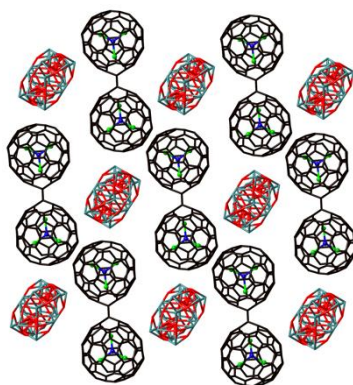
**Entry for the Table of Contents** (Please choose one layout)

Layout 1:

## COMMUNICATION

---

**Endohedral fullerene dimers** were formed upon reaction with a nickel telluride molecular cluster. The resulting solid state material assembled into a superatomic relative of the  $\text{Rb}_2\text{O}_2$  structure-type. The single-bonded endohedral fullerene dimer features a unique orientation of the encapsulated cluster.



*Anastasia A. Voevodin, Laura Abella, Edison Castro, Dr. Dan W. Paley, Prof. Dr. Luis M. Campos, Dr. Antonio Rodriguez-Forteza, Prof. Dr. Josep M. Poble, Prof. Dr. Luis Echegoyen, Prof. Dr. Xavier Roy*

**Page No. – Page No.**

**Dimerization of endohedral fullerene in a superatomic crystal**

WILEY-VCH

---